International Journal of Biological Macromolecules 47 (2010) 68–75

Contents lists available at ScienceDirect

International Journal of Biological Macromolecules

journal homepage: www.elsevier.com/locate/ijbiomac

Methyl thiophanate as a DNA minor groove binder produces MT–Cu(II)–DNA ternary complex preferably with AT rich region for initiation of DNA damage

Quaiser Saquib[a], Abdulaziz A. Al-Khedhairy[a], Saud A. Alarifi[a], Sansa Dutta[b], Swagata Dasgupta[b], Javed Musarrat[a,*]

[a] DNA Research Chair, Department of Zoology, College of Science, King Saud University, Riyadh 11451, Saudi Arabia
[b] Department of Chemistry, Indian Institute of Technology, Kharagpur 721302, India

ARTICLE INFO

Article history:
Received 5 January 2010
Received in revised form 6 March 2010
Accepted 29 March 2010
Available online 4 April 2010

Keywords:
Fungicide
Fluorescence quenching
Methyl thiophanate
Circular dichroism
Cyclic voltammetry
DNA binding

ABSTRACT

Interaction of a genotoxic fungicide methyl thiophanate (MT) has been studied in vitro with calf thymus DNA. Fluorescence quenching data revealed the binding constant ($K_a = 3.23 \times 10^4\ M^{-1}$) and binding capacity ($n = 1.1$) of MT with ctDNA. Ligand displacement studies using specific probes suggested the MT binding at DNA minor groove. The docking analysis further substantiated MT interaction with at least three AT base pairs within the DNA groove. A discernable change in E_0' value with decreased peak currents in cyclic voltammogram, and peak shifts in CD spectra reflected the formation of MT–ctDNA and MT–ctDNA–Cu(II) complexes. The results elucidate the significance of specific MT–DNA interactions as an initiating event in MT-induced DNA damage.

1. Introduction

Interactions of certain environmental genotoxicants and alkylating agents with cellular genome induce structural alterations in DNA molecule and cause detrimental effects on genetic regulatory circuit of the cell [1,2]. Covalent binding of such chemicals with DNA bases often forms pre-carcinogenic DNA adducts in animals and humans [3]. Amongst the environmental chemicals, certain pesticides have been categorized as potent genotoxicants and alkylating agents for DNA [4–6]. It is reported that the insecticides such as heptachlor, endosulfan, azinphos methyl, and imidacloprid interact with DNA and form promutagenic DNA adducts [7–9]. An insecticide carbofuran and diazinon has been reported to intercalate between the base pairs of ctDNA to form DNA–carbofuran and DNA–diazinon adducts [10,11]. All such pesticides, which either covalently bind or intercalate in DNA molecule and form DNA adducts may lead to gene mutations and initiate carcinogenesis, if the adducts are not repaired or misrepaired before DNA replication occurs [12]. Indeed, an increased DNA damage enhances the probability of mutations occurring in critical target genes and cells, which may enhance the process of carcinogenesis [13]. Several reports have suggested the possible link between pesticide-induced genotoxicity and damage to biological macromolecules in human population exposed to either single or mixture of pesticides [4,5,14].

In this study, a broad spectrum fungicide methyl thiophanate (MT) has been chosen as a ligand for in vitro DNA binding studies. MT is a known genotoxicant and our earlier studies have explicitly demonstrated its DNA damaging potential based on its ability to induce DNA strand breaks using single cell gel electrophoresis (Comet assay) and micronuclei (MN) assay in human lymphocytes [15]. It has also been shown to inflict oxidative damage in DNA and produces significant amount of reactive oxygen species [16]. However, to the best of our understanding in the light of available information, the mechanism of MT–DNA binding and its effect on DNA secondary structure have not been comprehensively pursued in a systematic manner. Thus, the sensitive techniques viz. fluorescence spectroscopy [10,11,17], circular dichroism [11,17–19] and cyclic voltammetry [11,20] have been employed for analyzing the in vitro interaction of MT with ctDNA. The study will address some pertinent and relatively unattended issues of fundamental significance, such as the (i) binding affinity and stoichiometry of DNA–MT complexation, (ii) probable region of MT binding on DNA, (iii) role of transition metal ion Cu(II) in forming the MT–Cu(II)–ctDNA ternary complex, and (iv) the plausible mechanism of MT binding with

* Corresponding author at: Al-Jeraisy Chair for DNA Research, Department of Zoology, College of Science, P.O. Box 2455, King Saud University, Riyadh 11451, Saudi Arabia. Tel.: +966 4675768; fax: +966 4675514.
E-mail address: musarratj1@yahoo.com (J. Musarrat).

0141-8130/$ – see front matter © 2010 Elsevier B.V. All rights reserved.
doi:10.1016/j.ijbiomac.2010.03.017

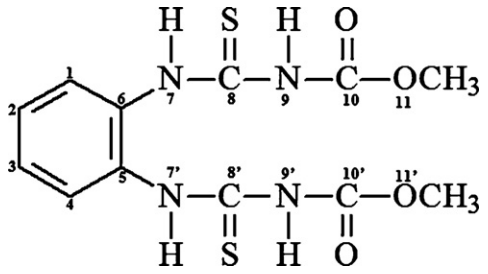

Fig. 1. Structure of methyl thiophanate (MT).

accessible nitrogenous bases, as an initiation event in the process of MT-induced genotoxicity.

2. Materials and methods

2.1. Chemicals

Calf thymus DNA (ctDNA), distamycine A (DistaA), ethidium bromide (EtBr), dimethyl sulfoxide (DMSO), Na_2–EDTA and Tris [hydroxymethyl] aminomethane were purchased from Sigma Chemical Company, St. Louis, MO, USA. The ctDNA was ethanol precipitated and dissolved in Tris–EDTA buffer pH 7.5. Its purity was determined by measuring absorption at 260 and 280 nm. The 260/280 ratio of 1.86 indicated that the ctDNA was sufficiently free of protein. The concentration of ctDNA was determined using an extinction coefficient of 6600 M^{-1} cm^{-1} at 260 nm. Methyl thiophanate (MT) 97% pure (Fig. 1) was obtained from Agrochemical Division, Indian Agriculture Research Institute (IARI, New Delhi, India). All experiments were done using MilliQ water.

2.2. MT–DNA binding analysis by fluorescence spectroscopy

The fluorescence quenching titration of MT with increasing ctDNA to MT molar ratios has been performed in a continuous manner. Briefly, to a fixed concentration of MT (50 μM), increasing concentrations of ctDNA (5–100 μM) were added to obtain the ctDNA to MT molar ratios from 0.1 to 2.0 in 10 mM Tris–HCl buffer at ambient temperature. The spectra were recorded under subdued light to prevent undesired photodegradation. Fluorescence measurements were carried out on a Shimadzu spectrofluorophotometer, model RF5301PC equipped with RF 530XPC instrument control software, using a quartz cell of 1 cm path length. The excitation and emission slits were set at 3 and 10 nm, respectively. The excitation and emission wavelengths at which the MT fluorescence recorded were 265 and 294 nm, respectively. ctDNA alone does not exhibit fluorescence at this wavelength range. Fluorescence quenching in terms of the quenching constant was determined following the Stern–Volmer Eq. (1) [21]:

$$\frac{F_0}{F} = 1 + K_{sv}[Q] \quad (1)$$

where F_0 and F are the fluorescence intensities in absence and presence of the quencher (ctDNA), respectively, K_{sv} is the Stern–Volmer quenching constant and [Q] the quencher concentration. The quenching constant was obtained from the slope of the Stern–Volmer plot (F_0/F versus [Q]). The binding constant (K_a) and number of binding sites (n) have been estimated, considering a 1:1 complex between MT and ctDNA, as described by Sahoo et al. [22], following the methods of Lehrer and Fasman [23], Chipman et al. [24], using Eq. (2):

$$\frac{F_0 - F}{F - F_\infty} = K_a \times [\text{DNA}] \quad (2)$$

where F_0 and F_∞ are the relative fluorescence intensities of MT alone and MT saturated with ctDNA (i.e. the relative fluorescence intensity of ctDNA to MT molar ratio of 1:2), respectively. The slope of the double-logarithm plot ($\text{Log}[(F_0 - F)/(F - F_\infty)]$) versus Log [ctDNA] in linear range provided the number of equivalent binding sites (n) however, the value of Log [ctDNA] at $\text{Log}[(F_0 - F)/(F - F_\infty)] = 0$ is equal to the negative logarithm of the binding constant (K_a) [25,21,22]. Also, the influence of divalent metal ion Cu(II) on the binding of MT–DNA was studied at the molar ratios of 1:0.2.

2.3. Fluorescence spectroscopic analysis of MT intercalation and minor groove binding on DNA

Binding specificity of MT as an intercalator or minor groove binder on B-DNA has been studied using ethidium bromide (EtBr), a well-known intercalator, and distamycine A (DistaA), a minor groove binder, as fluorescence probes [26,27]. EtBr–ctDNA complex at 1:5 molar ratio was excited at 545 nm in the absence and presence of MT at 1:5–20 molar ratios for EtBr displacement. The fluorescence measurement of DistaA–ctDNA complex (1:5 molar ratio) was performed at 320 nm and emission maxima recorded at 455 nm with the excitation and emission slits set at 5 and 10 mm, respectively. MT was added to the complex in increasing amounts to achieve the molar ratio range of 0.5–5.0 and scanned for competitive binding analysis.

2.4. Assessment of MT DNA binding with cyclic voltammetry

The redox potentials of the MT and MT–ctDNA complex in the absence and presence of Cu(II) were determined by cyclic voltammetry in an aqueous medium containing 0.4 M KNO_3, as a supporting electrolyte at room temperature. Cyclic voltammetric experiment was performed using an Electrochemical Analyzer (CH Instruments, Japan). A conventional three electrode system was employed with a platinum microcylinder as working electrode, platinum wire as an auxillary electrode and Ag/AgCl as a reference electrode. The formal potential $E_0'(E_{1/2})$ was taken as the average of the anodic (E_{pa}) and cathodic (E_{pc}) peak potentials.

2.5. Circular dichroism (CD) measurements

CD spectra of MT alone and in combination with ctDNA at a ratio of 1:5, in presence of 100 μM Cu(II) were obtained in a 1 cm path length cell. The CD measurements were carried out on Jasco spectropolarimeter, model J-815, Japan. The instrument was calibrated with d-10-camphorsulphonic acid. All the CD measurements were carried out at 25 °C with a thermostatically controlled cell holder attached to a NESLAB RTE-110 circulating water bath (NESLAB Instruments, Inc. USA) with an accuracy of ±0.1 °C. The spectra were collected at a scan speed of 100 nm per minutes with a response time of 1 s. Each spectrum was the average of four scans and corrected by subtraction of a buffered blank under identical conditions. The results expressed as CD[mdeg].

2.6. Docking analysis of MT–DNA Interaction

The B-DNA crystal structure used for the docking studies was obtained from the Protein Data Bank with identifier 453D [28]. The DNA file was prepared for docking by removing water molecules and adding polar hydrogen atoms with Gasteiger charges. The 3D structure of the ligand MT was generated in Sybyl 6.92 (Tripos Inc., St. Louis, USA) and its energy-minimized conformation was obtained with the help of the MMFF94 force field using MMFF94 charges. The rotatable bonds in the ligand were assigned with AutoDockTools and docking was carried out with the AutoDock 4.0

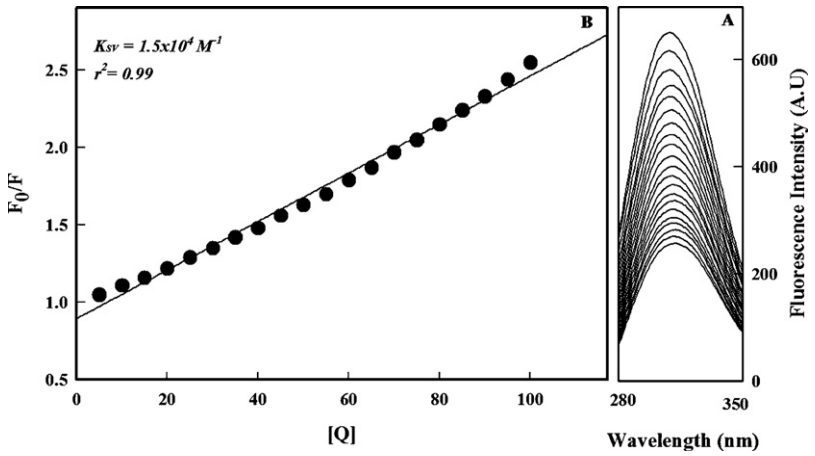

Fig. 2. Panel A depicts fluorescence emission spectra of MT in absence (uppermost curve) and presence of increasing amounts of ctDNA upon excitation of MT at 265 nm. The molar ratios of ctDNA to MT ranges from 0.1 to 2.0 (top to bottom). Panel B represents Stern–Volmer plot of MT–ctDNA fluorescence quenching data.

Lamarckian Genetic Algorithm (GA) [29,30]. DNA was enclosed in a grid having 0.375–0.431 Å spacing. Other miscellaneous parameters were assigned the default values given by AutoDock. The output from AutoDock was rendered in PyMol [31].

3. Results

3.1. Fluorescence quenching of MT upon binding with DNA

Fig. 2A shows the fluorescence emission spectra of MT and MT–ctDNA complex at an excitation wavelength of 265 nm. A significant decrease in the intrinsic fluorescence of MT with increasing ctDNA to MT molar ratios has been noticed. The data exhibited progressive quenching effect upon addition of ctDNA in increasing concentrations to a constant amount of MT, resulting in 61% fluorescence quenching at the highest ctDNA to MT molar ratios of 1:2.0. The plot of F_0/F versus [Q] (Fig. 2B) provided the quenching constant (K_{sv}) using Stern–Volmer algorithm as $1.5 \times 10^4\ M^{-1}$ ($r^2 = 0.99$). The fluorescence data plotted as Log $[(F_0 - F)/(F - F_\infty)]$ versus (Log [ctDNA]) in Fig. 3 revealed the binding constant (K_a) as $3.23 \times 10^4\ M^{-1}$ and (n) as 1.1. Fig. 4 shows the representative fluorescence emission spectra of MT in the absence and presence of 10 μM Cu(II) ions. Considering the fluorescence intensity value of MT alone as 100%, the extent of quenching at MT–Cu(II) molar ratio of 1:0.2 has been determined to be 9%. However, the intrinsic fluorescence of MT in combination with ctDNA alone and MT–ctDNA–Cu(II) decreased to the extents of 35.53 and 40.61%, respectively (Fig. 4). The results clearly exhibit more ctDNA–Cu(II) influenced MT fluorescence quenching as compared to ctDNA or Cu(II) alone.

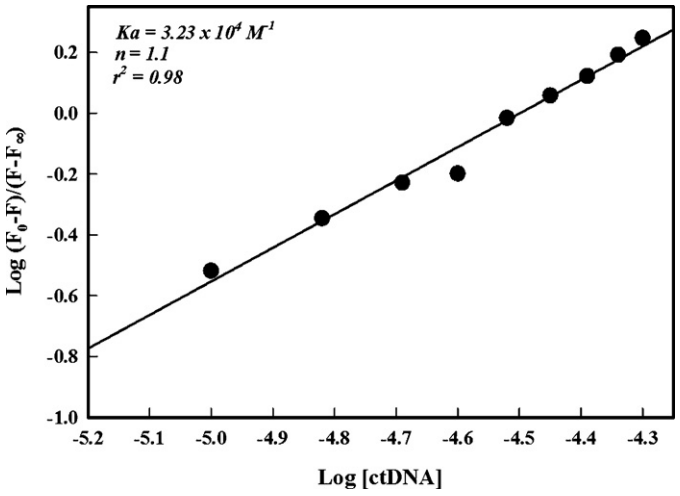

Fig. 3. The double-logarithmic plot of MT–ctDNA interaction to determine the binding constant (K_a) and number of binding sites (n).

3.2. DNA intercalation and minor groove binding of MT with DNA

Fig. 5 shows the effect of MT on the fluorescence intensity of EtBr–ctDNA complex 'in increasing molar ratio range of 1:5 to 1:20. Based on the observed fluorescence quenching, no significant displacement of EtBr bound to ctDNA has occurred even at the highest MT concentration, suggestive of non-intercalative mode of MT binding. Furthermore, the competitive binding has been performed with DistaA–ctDNA complex in order to determine the minor groove binding specificity of MT with DNA. The results shown in Fig. 6 indicate a gradual decline in the fluorescence emission spectra of DistaA–ctDNA complex at 455 nm with the addition

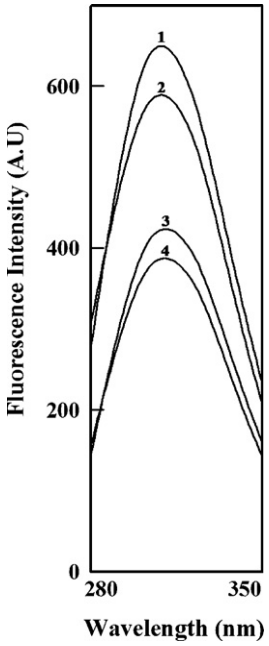

Fig. 4. Effect of Cu(II) on MT fluorescence. MT fluorescence was measured in absence and presence of 50 μM ctDNA and 10 μM Cu(II). (Curve 1) MT alone (50 μM), (curve 2) MT + Cu(II), (curve 3) MT + ctDNA and (curve 4) MT + ctDNA + Cu(II).

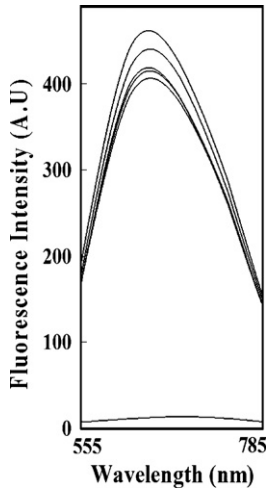

Fig. 5. Competitive displacement of intercalating dye ethidium bromide (EtBr) from EtBr–ctDNA complex by MT. Curves from top to bottom: EtBr (50 μM) + ctDNA (250 μM); EtBr (50 μM) + DNA (250 μM) + MT (250–1000 μM); EtBr alone (50 μM). The λ_{ex} and λ_{em} were 545 and 608 nm with slit apertures set at 1 and 1.5 nm, respectively.

of MT at increasing concentrations. Considering the fluorescence intensity value of DistaA–ctDNA and EtBr–ctDNA complexes as 100%, the extent of fluorescence quenching with MT have been determined to be 17.9 and 9.3% at the highest molar ratios of 1:5 and 1:20, respectively.

3.3. Voltammetric analysis of MT–DNA binding

Fig. 7 shows the interaction of MT with ctDNA and transition metal ion Cu(II) in aqueous medium containing 0.4 M KNO_3, as determined by cyclic voltammetry at ambient temperature within the sweep range from +0.2 V to −1.2 V. The cyclic voltammogram of the MT, as a ligand, exhibits a quasi-reversible redox peak with

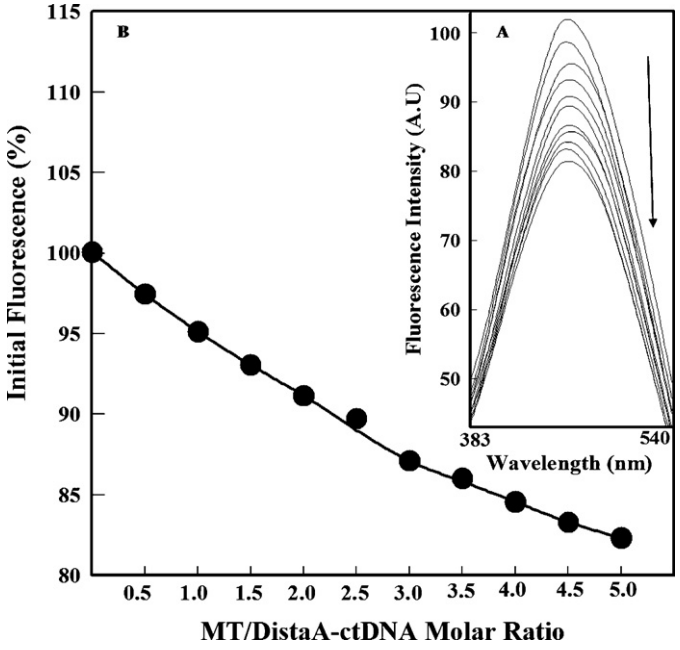

Fig. 6. Competitive binding of MT with ctDNA in presence of a minor groove binder DistaA. Fluorescence spectra in panel A represent the curves from top to bottom; DistaA–ctDNA complex (1:5), MT–ctDNA–DistaA molar ratios: 0.5, 1.0, 1.5, 2.0, 2.5, 3.0, 3.5, 4.0, 4.5 and 5.0. Panel B shows reduction in the initial fluorescence of DistaA–ctDNA complex with increasing molar ratios of MT.

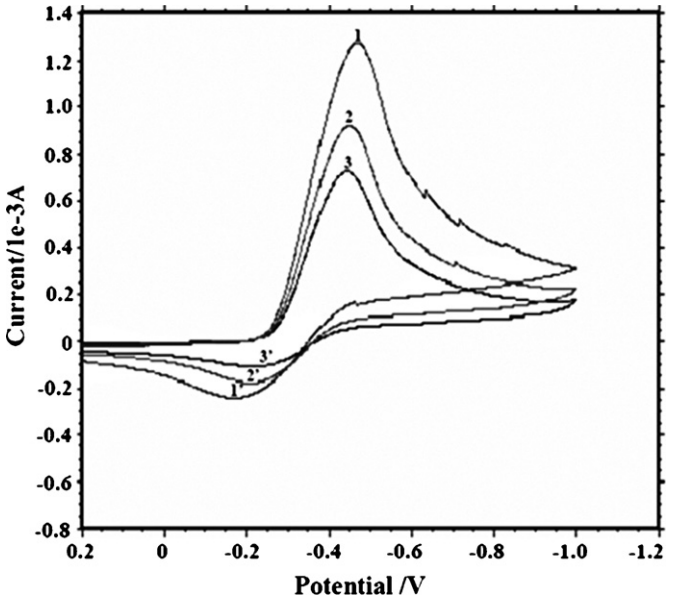

Fig. 7. Cyclic voltammograms showing typical Nernstian behavior of MT at a scan rate of 0.3 V s^{-1}. The peaks 1–3 represent: curve 1: MT (1 mM); curve 2: MT (1 mM) + ctDNA (1 mM); curve 3: MT + ctDNA + Cu(II) (1 mM each). The curves 1–3 and 1′ to 3′ represent the oxidation and reduction peaks, respectively.

ΔE_p value of 293 mV. Addition of ctDNA and ctDNA + Cu(II) to MT in solution reduces the ΔE_p values to 243 and 224 mV, respectively. The cathodic (i_{pc}) and anodic (i_{pa}) peak currents as well as the ratio of i_{pa}/i_{pc} also decreases, and the cathodic peak potential (E_{pc}) shifts towards less negative value. However, the anodic peak potential (E_{pa}) shifts towards a more negative value under identical conditions at a scan rate of 0.3 V s^{-1}. The formal potential, E_0' (or voltammetric $E_{1/2}$) taken as the average of E_{pc} and E_{pa} has been determined to be −0.317 with MT alone. Addition of ctDNA to MT solution at 1:1 molar ratio shifts the value of E_0' towards more negative potential.

3.4. Circular dichroism of MT–DNA–Cu(II) complex

The circular dichroism spectra of MT in the absence and presence of ctDNA and Cu(II) ions are shown in Fig. 8. The CD spectrum of MT shows the multiple positive bands at 205, 207, 210, 211, 214 and 216 nm, respectively. The addition of ctDNA to MT in equimolar

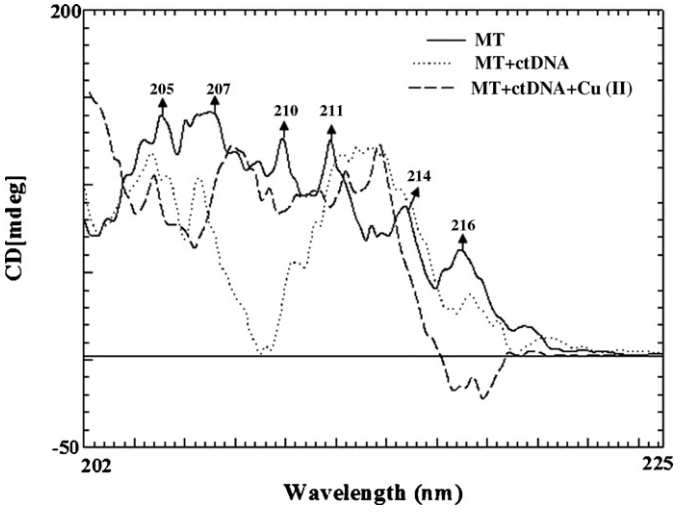

Fig. 8. CD spectra of MT in the absence and presence of ctDNA and Cu(II).

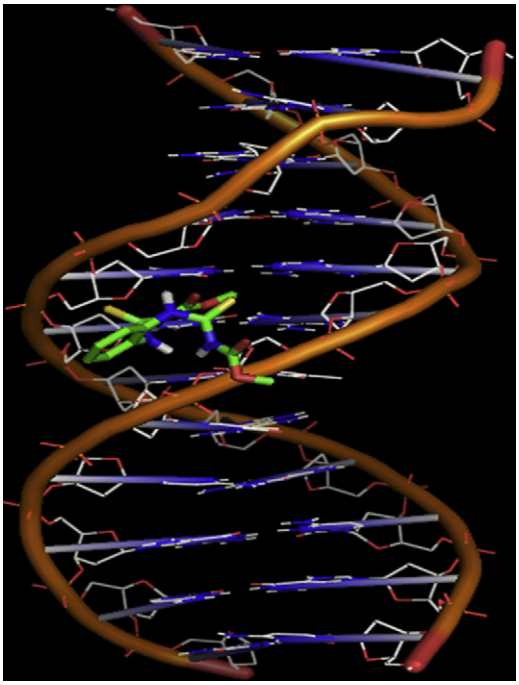

Fig. 9. Docking pose of energy-minimized structure of MT–ctDNA complex.

amount has resulted in the disappearance of peaks at positions 214 and 216 nm. Also, the peaks at 205, 207, 209 and 211 nm have exhibited a red shift by 1, 6, 8 and 9 nm, respectively. With the addition of Cu(II), the peaks at 205 and 209 nm have shown a red shift by 2 (+ve) and 8 (−ve) nm, respectively. While the peak at 207 nm, exhibited a red shift with the addition of ctDNA, resulting an appearance of two new peaks at 212 and 213 nm. MT peak at 211 nm has disappeared with the addition of Cu(II) and a prominent reduction in ellipticity occurred.

3.5. Molecular modeling of MT–DNA interaction

Molecular docking studies have been performed to substantiate the interaction and preferred binding mode of the ligand with DNA. Fig. 9 shows the docked conformation of the ligand MT with DNA. The docked structure revealed that the MT fits within the minor groove of DNA encompassing a length corresponding to ~3 base pairs. The distance of the ligand from the C-2 carbonyl oxygen of thymine (T) or the N-3 of adenine (A) shows the characteristic feature of minor groove binders. It is determined that the C-2 carbonyl oxygen of T-7 and T-8 is at a distance of 4.83 and 2.96 Å from 9-N and 11′-OCH_3 of MT. Moreover, the N-3 of A-18 and C-2 carbonyl oxygen of T-19 were at a distance of 2.62 and 4.39 Å of 11′-OCH_3 and 9-N of MT. The docking energy obtained was $-19\,kJ\,mol^{-1}$, which is slightly higher than the experimentally calculated free energy ($\Delta G = -25.2\,kJ\,mol^{-1}$) determined from the binding constant (K_a) value.

4. Discussion

Our earlier studies have demonstrated that the fungicide MT engender DNA strand breaks and produce reactive oxygen species in close proximity of DNA–MT complex. As to how and to what extent this genotoxic fungicide interacts with DNA is intriguing. Therefore, in order to elucidate the nature of MT–DNA complexation and the extent of binding, the interaction of MT with ctDNA has been investigated in this study, employing the sensitive analytical techniques. The extent and mode of MT binding with ctDNA have been ascertained by fluorescence measurements and DNA docking analysis. The fluorescence data revealed the quenching of intrinsic fluorescence of MT upon addition of ctDNA. Most likely this is due to masking of MT chromophore within the helix due to surface binding at the reactive nucleophilic sites on the heterocyclic nitrogenous bases of ctDNA molecule. Indeed, the quenching of fluorescence intensity of MT on addition of ctDNA is indicative of interaction. The fluorescence data suggested electrostatic interactions of MT with ctDNA resulting in the formation of MT–ctDNA binary complex. The quenching constant (K_{sv}) determined using the Stern–Volmer algorithm, signifies the affinity of this fungicide towards DNA. The plot of F_0/F vs. [Q] was not absolutely linear at higher complex concentrations and exhibited an upward curvature probably due to the high density of molecules in the system. Typically, the linearity of the Stern–Volmer plot suggests the (i) existence of one binding site for the ligand in the proximity of the fluorophore, or (ii) more than one binding site equally accessible to the ligand [32]. Thus, the gradual divergence from linearity of the Stern-Volmer plots on continuous addition of the ctDNA is suggestive of the presence of more than one binding site with different accessibilities and/or of the occurrence of combined static/dynamic quenching.

In order to elucidate the mode of interaction, the EtBr displacement with MT has been studied. EtBr is a well-known intercalator, which has been exploited as a spectral probe to explore the mode of binding of small molecules with DNA [33,26]. Owing to its planar structure, it binds to DNA in an intercalative fashion [34] and exhibits significant fluorescence enhancement on binding to double-stranded DNA [25]. However, if a test molecule is intercalative in nature, it may compete and decrease the binding sites available for EtBr, causing a concomitant reduction in fluorescence intensity of the EtBr-DNA complex. Wu et al. [26] have reported 50% decrease in the fluorescence intensity with the intercalator lucigenin. However, our data revealed that the addition of MT in increasing concentrations to EtBr–ctDNA complex does not exhibit a significant decrease in the fluorescence intensity of the complex. A meager 9.34% displacement of EtBr with MT at the highest molar ratio of 1:20, does not categorically signifies the MT intercalation into the ctDNA helix. Therefore, distamycin A (DistA), a polypyrrole antibiotic has been employed to assess the possible binding of MT at the ctDNA minor groove. DistaA is known to interact with the minor groove of B-DNA based on its curved shape, which matches well with the topology of double-stranded DNA. Thus, DistaA and its derivative compounds are referred as "shape-selective" binders [35]. Stockert et al. [36] have reported fluorescence enhancement of DistaA in aqueous solutions on binding to ctDNA in the minor groove. In this study, the DistaA–ctDNA complex showed significant quenching upon addition of MT. A gradual decline in the fluorescence intensity of the DistaA–ctDNA complex with the increasing molar ratios of MT suggested the possible displacement of DistaA and the formation of MT–ctDNA complex in the minor groove. MT is a benzimidazole class of compound and such interaction could be due to its structural similarity with other benzimidazoles, which are the known binders of DNA minor groove [27], which corroborates well with our findings. In general, the deeper and narrower minor groove of AT-rich sequences, and the absence of the protruding 2-amino group of guanine (G), is optimal for accommodating the shape of the compound and for maximizing the stabilized van der Waal's contacts. Hydrogen bonding between the groove floor base pairs and the linking amides and electrostatic stabilizing interactions with the protonated amines are primary contributors to the overall ligand–DNA stability. The thermodynamic parameters like changes in free energy (ΔG) due to ligand binding also provide an insight into the binding mode. Hydrogen bonds, van der Waals, hydrophobic and electrostatic interactions

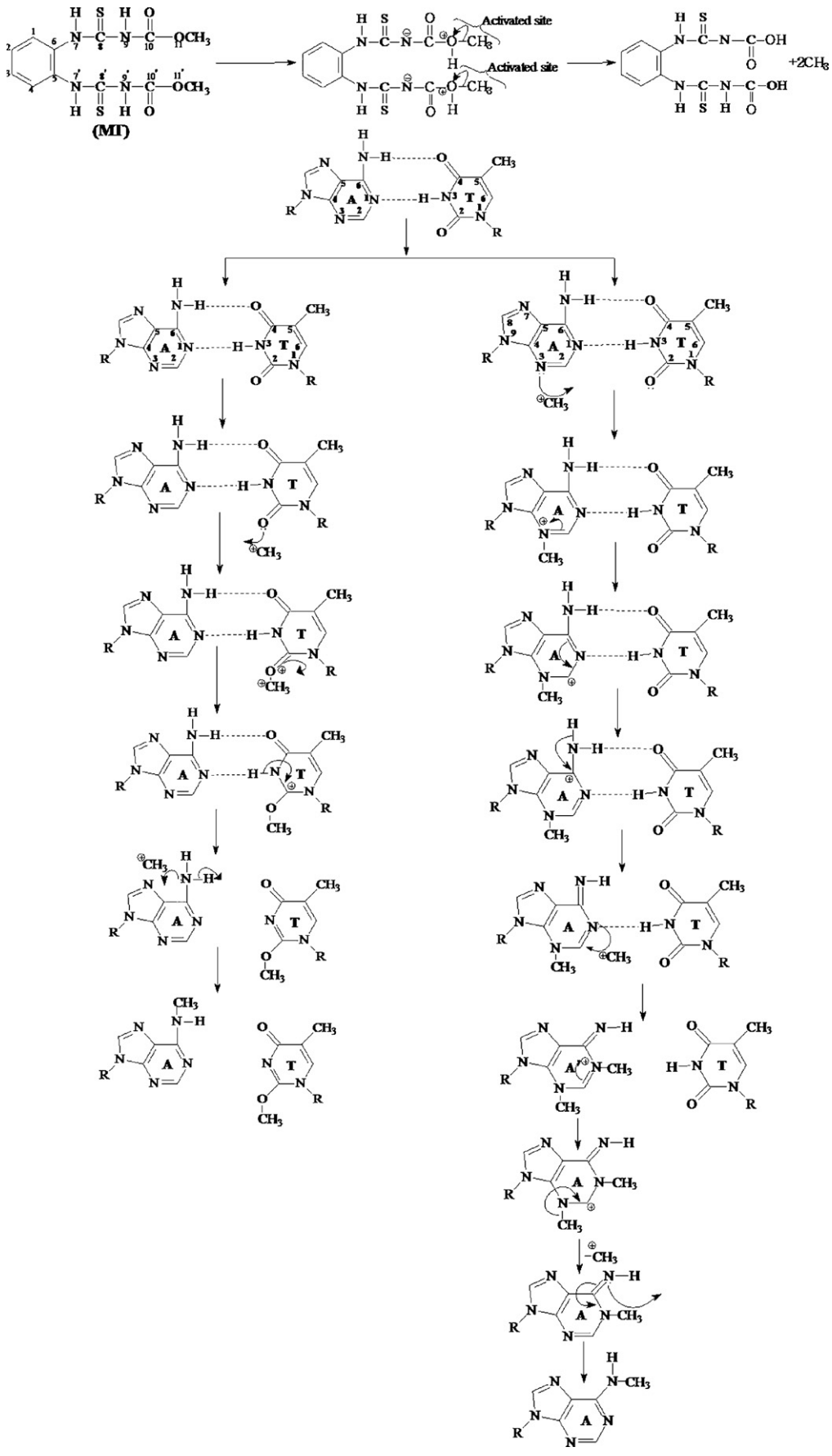

Scheme 1. Proposed mechanism of interaction of MT with AT base pairs in ctDNA.

are the major interactions that play a key role in molecular recognition [37]. The negative ΔG values for interaction of ctDNA with MT indicate the spontaneity of the complexation. The interaction process has been found to be entropy driven and the major contribution of ΔG comes from positive ΔS. For MT both the ΔH and ΔS (25.28 kJ mol^{-1} and 0.172 J mol^{-1}) were positive, which indicates that complexation between ctDNA and ligand also involve hydrophobic interactions. Addition of Cu(II) results in formation of MT–Cu(II)–ctDNA complex, which further augments the conformational changes by the local unwinding and may cause loss of helical integrity of duplex DNA.

The docking studies further substantiated the MT–ctDNA interaction. The docked structure revealed that MT could fit within the minor groove with a binding site of three base pairs long that preferably involves AT residues. A similar type of interaction has been reported with curcumin and diacetylcurcumin binding to ctDNA [38,22]. The minor groove-binding molecules generally have aromatic rings connected by single bonds that allow for torsional rotation in order to fit into the helical curvature of the groove with displacement of water molecules [39]. Thus, the narrower AT regions compared to G-C regions produce a better fit of these types of molecules into the minor groove and lead to van der Waals interactions with the DNA functional groups that define the groove. Hydrogen bonding from the C-2 carbonyl oxygen of T or the N-3 nitrogen of A to the minor groove binders is important [39]. Our results also showed the involvement of C-2 carbonyl oxygen of T-7, T-8, T-19 and N-3 of A-18 nitrogenous bases with N-9 and 11′-OCH_3 groups of MT, which explicitly suggest the preferential binding of MT to AT region in minor groove of DNA. Furthermore, the typical quasi-reversible redox peaks of cyclic voltammogram of the MT upon interaction with ctDNA and ctDNA–Cu(II) produced changes in the ΔE_p and E_0' values. The negative shift in formal potential (E_0') reflects that MT binding with ctDNA also involves electrostatic interactions. This finding corroborates well with the observations of Carter and Bard [40], who have reported electrostatic mode of interaction between small molecules and DNA, if E_0' shifts to a more negative value. However, if E_0' shifts to more positive value, the interaction mode is intercalative [10]. Nevertheless, the phenomena of the shift of E_0' and decrease of cathodic (i_{pc}) and anodic (i_{pa}) peak currents implied forming a new association complexes such as MT–ctDNA and MT–ctDNA–Cu(II).

The CD data exhibiting substantial changes in the ellipticity values clearly suggested the structural alterations and formation of MT–ctDNA–Cu(II) ternary complexes. These ternary complexes may indirectly enhance the surface binding of MT to ctDNA due to metal ion bridge formation. Our earlier studies [15] using Cu(I) specific chelating agent bathocuproine have demonstrated the significantly high binding of Cu(II) with MT, with subsequent reduction to Cu(I), which is known to form reactive oxygen species (ROS). It has been suggested that the formation of MT–Cu(II)–DNA ternary complex and consequent ROS generation, owing to Cu(II)/Cu(I) redox cycling in DNA proximity, is an important factor responsible for MT-induced DNA damage [15]. Cooper is considered as one of the major metals present in the nucleus [41] and its concentration in tissues ranges from 10 to >100 μM [42]. Thus, the interaction data reflecting spectral changes in the MT upon binding with ctDNA and Cu(II) ions, elucidate the significance of MT, ctDNA and Cu(II) interactions related to genotoxicity and cytotoxicity. A theoretical model presented as Scheme 1 depicts the possibility of methyl group ($^+CH_3$) transfer from MT to DNA bases. Our earlier studies have also reported the development of transient activated groups during the formation of stable MT–Cu(II) complex [15]. In all likelihood, the basic chemistry involved in the interaction process is the transfer of free lone pair of electrons, at neutral pH, at the reactive C-10, C-10′ and N-9, N-9′ positions on the bilaterally symmetrical arms attached to the aromatic ring of MT, which facilitates the release of methyl cations. The methyl moieties could be preferentially trapped at the nucleophilic centers N-6 and N-3 of A and C-2 carbonyl oxygen of T. The addition of methyl group to the nitrogenous base perturbs their aromatic character, causing hydrogen bond breakage and consequent GC to AT mispairing. The suggested alkylation at N-3, N-6 and C-2 carbonyl oxygen positions of A and T, respectively could be an additional factor promoting MT genotoxicity. Thus, it is concluded that the MT binds to DNA with sufficiently high affinity to cause MT–DNA, MT–DNA–Cu(II) complexation, and DNA alkylation. Formation of these adducts is envisaged as an initiating step in triggering MT-induced DNA damage, which if not processed by cellular DNA repair machinery may have genotoxic and carcinogenic implications.

Acknowledgement

Financial support through the DNA Research Chair, King Saud University, Riyadh, for completing this work is greatly acknowledged.

References

[1] L.R. Shugart, in: V.E. Forbes (Ed.), Genetics and Ecotoxicology, Taylor & Francis Publishers, Philadelphia, 1998, pp. 151–168.
[2] V. Tembe, B.R. Henderson, Cell. Signal. 19 (2007) 1113–1120.
[3] K. Hemminki, Carcinogenesis 14 (1993) 2007–2012.
[4] P. Padmavathi, P.A. Prabhavathi, P.P. Reddy, Bull. Environ. Contam. Toxicol. 64 (2000) 155–160.
[5] D. Zeljezic, V. Garaj-Vrhovac, Chemosphere 46 (2002) 295–303.
[6] Y. Cui, J. Guo, B. Xu, Z. Chen, Mutat. Res. 604 (2006) 36.
[7] M. Dhouib, A. Pfohl-Leszkowicz, G. Dirheimer, A. Lugnier, Toxicol. Lett. 78 (1995) 28–29.
[8] A. Laouedj, C. Cschenk, A. Pfohl-leszkowicz, G. Keith, D. Schontz, P. Guillernaut, B. Dether, Environ. Pollut. 90 (1995) 409–414.
[9] R.G. Shah, J. Lagueux, S. Kapur, P. Levallois, P. Ayoote, M. Tremblay, J. Zee, G.G. Poirier, Mol. Cell. Biochem. 169 (1997) 177–184.
[10] L.J. Zhang, S.G. Min, G.X. Li, Y.M. Xiong, Y. Sun, Guang Pu Xue Yu Guang Pu Fen Xi 25 (2005) 739–742.
[11] S. Kashanian, M.B. Gholivand, F. Ahmadi, H. Rava, DNA Cell Biol. 27 (2008) 1–7.
[12] R.C. Gupta, G. Spencer-Beach, Regul. Toxicol. Pharmacol. 23 (1996) 14–21.
[13] G. Eisenbrand, B. Pool-Zobel, V. Baker, M. Balls, B.J. Blaauboer, A. Boobis, A. Carere, S. Kevekordes, J.C. Lhuguenot, R. Pieters, J. Kleiner, Food Chem. Toxicol. 40 (2002) 193–236.
[14] V. Garaj-Vrhovac, D. Zeljezic, Toxicology 165 (2001) 153–162.
[15] Q. Saquib, A.A. Al-Khedhairy, S. Al-Arifi1, A. Dhawan, J. Musarrat, Toxicol. In vitro 23 (2009) 848–854.
[16] Q. Saquib, A.A. Al-Khedhairy, B.R. Singh, J.M. Arif, J. Musarrat, J. Environ. Sci. Health B 45 (2010) 40–45.
[17] M.A. Khan, J. Musarrat, Int. J. Biol. Macromol. 33 (2003) 49–56.
[18] Y. Zhu, G. Cheng, S. Dong, Biophys. Chem. 87 (2000) 103–110.
[19] W. Zhong, J.S. Yu, Y. Liang, K. Fan, L. Lai, Spectrochim. Acta A 60 (2004) 2985–2992.
[20] S.F. Wang, T.Z. Peng, C.F. Yang, J. Electroanal. Chem. 544 (2003) 87–92.
[21] J.R. Lakowicz, Principles of Fluorescence Spectroscopy, Third ed., Springer, New York, 2006.
[22] B.K. Sahoo, K.S. Ghosh, R. Bera, S. Dasgupta, Chem. Phys. 351 (2008) 163–169.
[23] S.S. Lehrer, G.D. Fasman, Biochem. Biophys. Res. Commun. 23 (1966) 133–138.
[24] D.M. Chipman, V. Grisaro, N. Sharon, J. Biol. Chem. 242 (1967) 4388–4394.
[25] J.L. Bresloff, D.M. Crothers, Biochemistry 20 (1981) 3547–3553.
[26] H.L. Wu, W.Y. Li, X.W. He, K. Miao, H. Liang, Anal. Bioanal. Chem. 373 (2002) 163–168.
[27] S.M. Nelson, L.R. Ferguson, W.A. Denny, Mutat. Res. 623 (2007) 24–40.
[28] H.M. Berman, J. Westbrook, Z. Feng, G. Gilliland, T.N. Bhat, H. Weissig, I.N. Shindyalov, P.E. Bourne, Nucleic Acids Res. 28 (2000) 235–242.
[29] G.M. Morris, D.S. Goodsell, R. Huey, A.J. Olson, J. Comput. Aided Mol. Des. 10 (1996) 293–304.
[30] G.M. Morris, D.S. Goodsell, R.S. Halliday, R. Huey, W.E. Hart, R.K. Belew, A.J. Olson, J. Comput. Chem. 19 (1998) 1639–1662.
[31] W.L. DeLano, The PyMOL Molecular Graphics System, DeLano Scientific, San Carlos, CA, USA, 2004, http://pymol.sourceforge.net.
[32] K.S. Ghosh, B.K. Sahoo, D. Jana, S. Dasgupta, J. Inorg. Biochem. 102 (2008) 1711–1718.
[33] J.B. LePecq, C. Paoletti, J. Mol. Biol. 27 (1967) 87–106.
[34] S. Satyanarayana, J.C. Dabrowiak, J.B. Chaires, Biochemistry 31 (1992) 9319–9324.
[35] W.C. Tse, D.L. Boger, Chem. Biol. 11 (2004) 1607–1617.
[36] J.C. Stockert, P. Del Castillo, J.L. Bella, Histochemistry 94 (1990) 45–47.

[37] P.D. Ross, S. Subramanian, Biochemistry 20 (1981) 3096–3102.
[38] F. Zsila, Z. Bikádi, M. Simonyi, Org. Biomol. Chem. 2 (2004) 2902–2910.
[39] R.B. Silverman, The Organic Chemistry of Drug Design and Drug Action, Second ed., Elsevier, New York, 2004.
[40] M.T. Carter, A.J. Bard, J. Am. Chem. Soc. 111 (1989) 8901–8911.
[41] S.E. Bryan, Metal Ions in Biological System, Marcel Dekker, New York, 1979.
[42] M.C. Linder, Nutritional Biochemistry and Metabolism, Elsevier Science, New York, 1991.